Journal of Physics: Conference Series **2533** (2023) 012044 doi:10.1088/1742-6596/2533/1/012044

Axion like particles, fifth force and neutron interferometry

Antonio Capolupo

Dipartimento di Fisica "E.R. Caianiello" Università di Salerno, and INFN — Gruppo Collegato di Salerno, Via Giovanni Paolo II, 132, 84084 Fisciano (SA), Italy

Salvatore Marco Giampaolo

Institut Ruder Boskovic, Bijenicka cesta 54, 10000 Zagreb, Croatia

Aniello Quaranta

Dipartimento di Fisica "E.R. Caianiello" Università di Salerno, and INFN — Gruppo Collegato di Salerno, Via Giovanni Paolo II, 132, 84084 Fisciano (SA), Italy

Abstract.
We report on recent result according to which the fermion-fermion interaction mediated by axions and axion–like particles can be revealed by means of neutron interferometry. We assume that the initial neutron beam is split in two beams which are affected by differently oriented magnetic fields, in order that the phase difference depends only by the axion–induced interaction. In this way, the phase difference is directly related to the presence of axions.

Phenomena, ranging from neutrino mixing [1, 2, 3, 4, 5, 6, 7] to the dark matter and energy [8, 9], to the muon g-2 anomaly [10, 11], together with the strong CP problem (i.e. the absence of CP symmetry violation in strong interaction, solved by Peccei and Quinn [12, 13] by introducing pseudo–scalar particles known as axions [12, 13, 14, 15, 16]) show the necessity of physics beyond the standard model of particles [17]. Axions and axion–like particles (ALPs) [18, 19, 20, 21, 22], with masses from the ultralight [23, 24] $m \simeq 10^{-22}$eV to the heavy axions [25] $m \simeq 1$ TeV, could represent a possible dark matter component [26]. Many experiments searched for ALPs [27, 28, 29, 30, 31, 32, 33, 34, 35], however, up to now no evidence for ALPs has been found. ALPs interact with the electromagnetic field, moreover, they are expected to play the role of a mediating boson in the fermion–fermion interaction [36, 37]. Therefore, different experiments were designed to probe such interactions [38, 40, 39, 41].

Another extremely thriving field of physics is the neutron interferometry [42]. It has allowed to verify many theoretical effects, such as the Sagnac effect [43], the geometric phase [44, 45, 46] and the wave–particle duality.

Here, we report on a new approach to detect ALPs, which suggests the use of a neutron interferometer in which two sub–beams are subject to external magnetic fields of equal strength but different direction, as a device to reveal fermion-fermion interaction mediated by axions. [47]. Indeed, we show that a detectable neutron phase difference, depending only by the axion–induced interaction between neutrons, can be achieved by setting the magnetic fields in the arms of the interferometer, one in the direction of propagation of the relative sub-beam and the other

Journal of Physics: Conference Series 2533 (2023) 012044 doi:10.1088/1742-6596/2533/1/012044

one orthogonally to the propagation. We fix the experimental parameters in order that the phase difference depends only on the axion–mediated interaction and the contributions given by the other interactions are removed. Then we show how a neutron interferometer is sensible to the presence of ALPs in a significant portion of parameter space.

The Lagrangian describing the neutron-neutron interaction due to axion exchange is given by [36, 37]

$$\mathcal{L}_{INT} = -\sum_{j=1,2} i g_{aj} \phi \bar{\psi}_j \gamma_5 \psi_j \tag{1}$$

with ϕ the axion field, ψ_1, ψ_2 fermion fields and g_{aj} the (dimensionless) effective axion–fermion coupling constants, $g_{aj} = g_{aNN}$ in the case of axion-neutron coupling. Such constant is depending on the axion (or ALP) model and on the fermions interacting. We shall assume that the neutron velocities are non-relativistic and analyze this interaction potential within the context of ordinary quantum mechanics. In the non–relativistic limit $\mathcal{L}_{INT}$ yields a two–body potential for the neutrons [36, 37]. This axion–induced interaction is not the only one in play. However, the gravitational interaction is easily seen to be irrelevant, due to the smallness of the masses involved. In addition, we shall always assume a relative distance $r > 10^{-12}m$ among the neutrons, so that the short–range nuclear interactions can also be ignored. With this assumption the only other relevant interaction is the magnetic one between the neutron dipoles. The neutron–neutron interaction Hamiltonian comprising the magnetic and the axion–mediated interaction, generalized to an arbitrary number of neutrons can be written as [47]

$$H_{ij} = -\frac{\mathcal{A}}{r_{ij}^3}\left[\left(3 - \mathcal{B}e^{-mr_{ij}}K^{(a)}(r_{ij})\right)\sigma_i^{r_{ij}}\sigma_j^{r_{ij}} - \left(1 - \mathcal{B}e^{-mr_{ij}}K^{(b)}(r_{ij})\right)\boldsymbol{\sigma}_i \cdot \boldsymbol{\sigma}_j\right]. \tag{2}$$

In eq. (2) the two contributions are signaled by the parameters $\mathcal{A} = \frac{g^2\alpha}{16M^2}$, denoting the strength of the magnetic interaction (g is the neutron g–factor, M is the neutron mass and α is the fine-structure constant) and $\mathcal{B} = \frac{g_{aNN}^2}{\pi\alpha g^2}$, representing the relative weight of the axion interaction, which vanishes in absence of the ALP (whose mass is denoted m). The dimensionless (in natural units $c = 1 = \hbar$) functions $K(r)$ are defined as $K^{(a)}(r) = m^2r^2 + 3mr + 3$, and $K^{(b)}(r) = mr + 1$. The vector $\boldsymbol{r_{ij}} = \boldsymbol{r_i} - \boldsymbol{r_j}$ denotes the relative position of the neutrons i and j, $r_{ij} = |\boldsymbol{r_{ij}}|$ is their relative distance and the operators $\sigma_l^{r_{ij}} = \boldsymbol{\sigma}_l \cdot \boldsymbol{\hat{r}_{ij}}$ are defined by the projection of the pauli operators $\boldsymbol{\sigma_l}$ of neutron l on $\boldsymbol{r_{ij}}$. The notation $\sigma_i^{r_{ij}}$ is used to remark that while these operators act only upon the space of the i-th particle, their form depends on the specific pair i, j considered. Eq.(2) can be recast in a more compact form by defining the functions $C(r) = \frac{\mathcal{A}}{r^3}\left(1 - \mathcal{B}e^{-mr}K^{(b)}(r)\right)$, $D(r) = \frac{\mathcal{A}}{r^3}\left(3 - \mathcal{B}e^{-mr}K^{(a)}(r)\right)$ and the symmetric matrix $K^{uv}(\boldsymbol{r}) = C(r)\delta^{uv} - D(r)R^u(\boldsymbol{r})R^v(\boldsymbol{r})$ for $u, v = x, y, z$. The symbol $R^u(\boldsymbol{r}) = \boldsymbol{\hat{r}} \cdot \boldsymbol{\hat{u}}$ denotes the projection of the vector $\boldsymbol{r}$ on the u axis. Thus $H_{ij} = \sum_{u,v} K^{uv}(\boldsymbol{r}_{ij})\sigma_i^u\sigma_j^v$. The two–neutron interaction can easily be generalized to an arbitrary number of neutrons. The total interaction Hamiltonian is simply the sum over all pairs i, j $H = \frac{1}{2}\sum_{i,j} H_{ij}$, where the factor $\frac{1}{2}$ accounts for double counting.

The study of the evolution of the n–neutron states interacting via H represents a complicated many–body problem. However, we want to consider only the evolution of the single neutron state and we are not interested to correlations and collective effects. Therefore, by using a mean field approach, we describe the interaction of a neutron with all the other nucleons by means of an effective one–particle potential. Let us consider a neutron at position $\boldsymbol{r}_i$ and the Pauli operator $\boldsymbol{\sigma}_i$, the instantaneous interaction hamiltonian due to the other neutrons is $H_i = \sum_{u,v}\sum_{j\neq i} K^{uv}(\boldsymbol{r}_{ij})\sigma_j^u\sigma_i^v$, where the sum is relative to all the other neutrons j. Since we are interested to an effective local potential for the single neutron, then we substitute the above equation with its expectation value on the state of the other nucleons. Notice that the term of a spin interacting with a magnetic field $H_i = -\mu\left(\boldsymbol{B_i}(\boldsymbol{r_i})\right)\cdot\boldsymbol{\sigma}$, is obtained by setting

$$\mu\boldsymbol{B_i}(\boldsymbol{r_i}) = -\sum_u\sum_j K^{uv}(\boldsymbol{r_{ij}})\langle\sigma_j^u\rangle\,. \tag{3}$$

The evolution of the single neutron state is analyzed by determining the effective magnetic field for a particular spatial spin configuration, and then by inserting the one particle operator into the Schroedinger equation.

For our purposes, we shall consider cold neutron beams with specific requirements. First of all, we deal with collimated neutron beams and a small beam width of the order of 10 μm. Experimentally, such kind of beams can be produced in different ways as shown in [48]. Neglecting the angular spread, we can assume that the beam is distributed with cylindrical symmetry around the beam axis $\hat{\boldsymbol{y}}$, and, considering it sufficiently thin, we can represent the beam as a monodimensional system. We will also assume that, by using a monochromator, one can select only neutrons around a given value of the kinetic energy K. The beam intensity is expected to decay as the neutron beam propagates. However, as a first instance, we consider the beam intensity constant and neglect the losses due to the propagation.

We now present, in Fig.(1), the scheme of the neutron interferometer eligible for the detection of the axion–mediated interaction among fermions. In such a scheme, a source, as a reactor, **SRC** generates cold or ultra–cold neutrons, which are directed to monochromator and a collimator **EXT**, making the beam (approximately) linear and monochromatic. Then a beam splitter **BS** separates the beam into two sub–beams I and II which enter in a device that selects two different spin polarizations $\boldsymbol{P}_I$ and $\boldsymbol{P}_{II}$. The sub–beams pass through regions permeated by magnetic fields of the same strength but with distinct direction, i.e. $\boldsymbol{B^0_J} = B_0\boldsymbol{P_J}$.

Making as close as possible the fractional intensities of the sub-beams χ_J with respect to the initial beam I_0: $\chi_J = I_J/I_0$, $J = I, II$, $\chi_I \simeq \chi_{II}$, one has that the average distances between successive neutrons in the two sub–beams are similar $d_I \simeq d_{II}$. Indeed, $d_J = \frac{\bar{v}_J}{I_J}$, with $\bar{v}_J$ average neutron velocity of propagation in the J sub–beam. Moreover, considering constant I_J and $\bar{v}_J$, the distances d_J are constant, and the one particle Hamiltonian H is time–independent. We assume that $d_J > 10^{-12}m$ in order that the effects of nuclear interactions are negligible.

The interference is detected in a plane **IP** where the polarized sub–beams hit, after crossing two optical paths of the same length

We choose $\boldsymbol{P}_I$ to be orthogonal to $\hat{\boldsymbol{y}}_I$ and $\boldsymbol{P}_{II}$ parallel to $\hat{\boldsymbol{y}}_{II}$. Starting from the total interaction Hamiltonian, exploiting the assumption that all the distances between two subsequent neutrons in sub–beam J are equal to d_J, with simple algebraic steps, one arrives at the effective magnetic fields [47]. It is easy to show that, within these assumptions, each neutron in sub–beam J is subject to the same effective magnetic field $\mu\boldsymbol{B_J} = \mu B_J\boldsymbol{P_J}$ given by

$$\begin{aligned}
\mu B_I &= -\frac{2\mathcal{A}\zeta(3)}{d_I^3} + \frac{2\mathcal{AB}}{d_I^3}\mathrm{Li}_3(e^{-md_I}) + \frac{2\mathcal{AB}m}{d_I^2}\mathrm{Li}_2(e^{-md_I}) \\
\mu B_{II} &= \frac{4\mathcal{A}\zeta(3)}{d_{II}^3} - \frac{4\mathcal{AB}}{d_{II}^3}\mathrm{Li}_3(e^{-md_{II}}) - \frac{4\mathcal{AB}m}{d_{II}^2}\mathrm{Li}_2(e^{-md_{II}}) \\
&\quad + \frac{2\mathcal{AB}m^2}{d_{II}}\log(1 - e^{-md_{II}})
\end{aligned} \tag{4}$$

where $\zeta(s)$ stands for the Riemann zeta function while $\mathrm{Li}_s(z) = \sum_{n=1}^{\infty}\frac{z^n}{n^s}$ is the Polylogarythm function [49]. The Schroedinger equation ruling the evolution of the single neutron state, in both sub–beams, is

$$i\partial_t\psi_J = \left(-\frac{\nabla^2}{2M} + M\right)\psi_J - \boldsymbol{\sigma}\cdot\left[\mu(\boldsymbol{B_J} + \boldsymbol{B^0_J})\right]\psi_J \tag{5}$$

Journal of Physics: Conference Series **2533** (2023) 012044 doi:10.1088/1742-6596/2533/1/012044

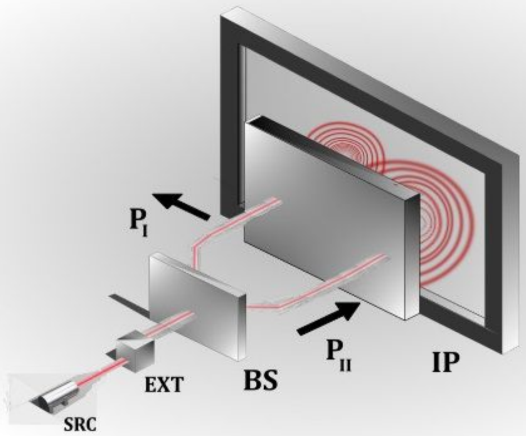

Figure 1. (color online) Diagram of the interferometric apparatus. The beam from the neutron source **SRC** is transmitted to a collimation device and a monochromator **EXT**. Then the beam is conveyed to a beam splitter **BS** which splits the beam into two subbeams with different average spin polarizations $\boldsymbol{P}_I$ and $\boldsymbol{P}_{II}$. In the end, the two subbeams interfere at the interference plane **IP**.

with ψ_J the product of a spatial wave-function and a spin function. We express the spinor for each sub–beam in the basis defined by the corresponding polarization, i.e. $\boldsymbol{\sigma}\cdot\boldsymbol{P_J}|\uparrow_J\rangle = |\uparrow_J\rangle$ and $\boldsymbol{\sigma}\cdot\boldsymbol{P_J}|\downarrow_J\rangle = -|\downarrow_J\rangle$. Moreover, we assume that the neutron, after passing the beam splitter, is in the up state for the corresponding sub–beam. We consider $t = 0$ at this instant. Denoting with y the coordinate along the propagation axis, with $y = 0$ and $t = 0$ at the beginning of the optical path, one has $\psi_J(t) = f(t)e^{iky}|\uparrow_J\rangle$ with $f(t)$ a function which can be assumed as $f(t) = e^{-i\omega_J t}$. Then, from Eq.(5) we have $\omega_J = \frac{k^2}{2M} + M - \mu B_J - \mu B_0$, and the total phase at time t is given by $\phi_J(t) = \arg\left(\langle\psi_J(0)|\psi_J(t)\rangle\right) = -\left(\frac{k^2}{2M} + M - \mu(B_J + \mu B_0)\right)t$. The phase difference between the two beams at time t is $\Delta\phi(t) = \phi_{II}(t) - \phi_I(t) = \mu\left(B_{II} - B_I\right)t$, where μB_I and μB_{II} are given in Eq. (4). By setting $d_I = d_{II} = d$, $\Delta\phi(t)$ can be written as $\Delta\phi(t) = \left[G_m(d) + G_a(d)\right]t$, where $G_m(d) = \frac{6\mathcal{A}}{d^3}\zeta(3)$ is due to the dipole–dipole interaction and

$$G_a(d) = -\frac{6\mathcal{A}\mathcal{B}}{d^3}\mathrm{Li}_3(e^{-md}) - \frac{6\mathcal{A}\mathcal{B}m}{d^2}\mathrm{Li}_2(e^{-md}) + \frac{2\mathcal{A}\mathcal{B}m^2}{d}\log(1 - e^{-md}) \,,$$

is due to the axion–mediated interaction. Here the $n \to \infty$ limit is intended.

Neglecting a possible phase shift due to the beam splitter, the phase difference induced by the dipole-dipole interactions can be removed by setting the beam path in such a way that $G_m(d)$ is an integer multiple of 2π. This is obtained for time intervals T_k, which for any integer k are $T_k = \frac{2k\pi}{G_m(d)} = \frac{k\pi d^3}{3\mathcal{A}\zeta(3)}$. The phase difference, evaluated at T_k, is then

$$\Delta\phi(T_k) \quad = \quad \left\{\frac{k\pi\mathcal{B}}{3\zeta(3)}\left[2m^2d^2\log(1 - e^{-md}) - 6md\mathrm{Li}_2(e^{-md}) - 6\mathrm{Li}_3(e^{-md})\right]\right\}_{\mathrm{mod}\,2\pi}, \qquad (6)$$

and it is different from zero only in presence of ALPs. Indeed, $\Delta\phi(T_k) = 0$ for $\mathcal{B} = 0$. Eq.(6) shows that $\Delta\phi(T_k)$ is proportional to the parameter $\mathcal{B} \propto g_p^2$. For ALP masses $m \in [10^{-6} - 1]$eV, and distances $d \in [10^{-11} - 10^{-6}]$m, one has that $\Delta\phi(T_k)$ depends only weakly on m and d, while it depends strongly on the coupling. The phase difference, modulo 2π, is plotted in Fig.(2), at the minimum recurrence time T_1, for several values of the coupling constant g_p in the mass range $[10^{-3}, 1]$ eV. For axion masses $m < 0.1$eV, one has that $\Delta\phi$ is almost independent on the distance for $d = 10^{-8}$m and $d = 10^{-6}$m. The dependence on the distance is relevant only when

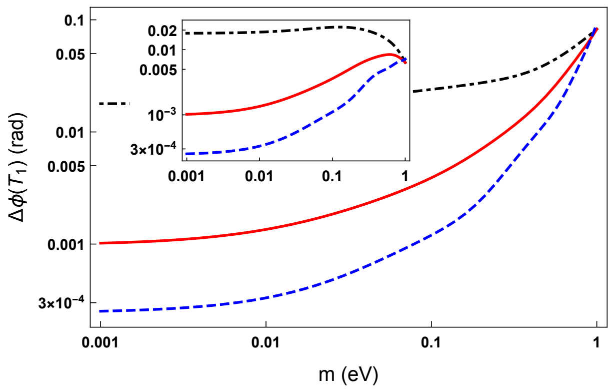

Figure 2. (color online) Logarithmic scale plot of the phase difference $|\Delta\phi(T_1)|$ modulo 2π for several values of the coupling constant in the ALP mass range $[10^{-3}, 1]$ eV for an inter–neutron distance $d = 10^{-8}$m ($d = 10^{-6}$m in the inset). In particular: the black dot–dashed line is obtained by considering the threshold from effective Casimir pressure measurements [38], $g_p = g_{CP}$, and using the following values $g_{CP} = 0.0327$ for $m = 10^{-3}$eV, $g_{CP} = 0.0348$ for $m = 0.05$eV, $g_{CP} = 0.0674$ for $m = 1$eV. For the red solid line, we used $g_p = g_{CF}$, where g_{CF} is the threshold from measurements of the difference of Casimir forces [39] and the sample values are $g_{CF} = 0.007$ for $m = 10^{-3}$eV, $g_{CF} = 0.012$ for $m = 0.05$eV, $g_{CF} = 0.066$ for $m = 1$eV. In the blue dashed line we assume $g_p = g_{IE}$, where g_{IE} is the threshold from isoelectronic experiments [40], and sample values are $g_{IE} = 0.0036$ for $m = 10^{-3}$eV, $g_{IE} = 0.006$ for $m = 0.05$eV, $g_{IE} = 0.07$ for $m = 1$eV.

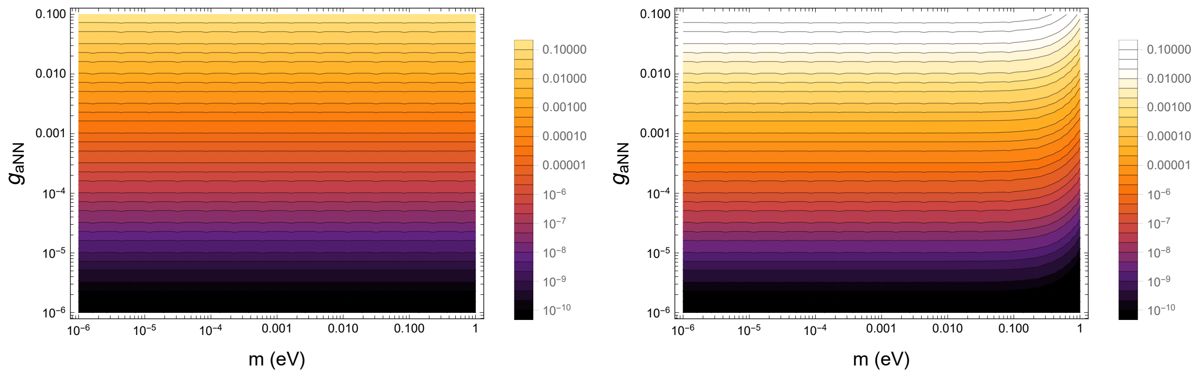

Figure 3. (color online) Contour plots of $|\Delta\phi(T_1)|$ in the mass–coupling plane for $d = 10^{-9}m$ (left panel) and $d = 10^{-6}m$ (right panel). The range of axion masses and coupling constant adopted is $(m, g_p) \in [10^{-6}, 1]\text{eV} \times [10^{-6}, 10^{-1}]$.

the product md is quite high. On the other hand, for $md \ll 1$, $\Delta\phi$ essentially depends only on the coupling g_p.

The plots of Fig.(3) show the g_p^2 dependence of $\Delta\phi(T_1)$ and an extremely weak dependence on the ALP mass in the ranges analyzed.

Notice that in order to detect the phase difference, one has to take into account the limitation coming from the need for a recurrence time T required to isolate the axion contribution to $\Delta\phi$, and the limitation due to the total neutron flux available, which is fundamental for a sufficient small inter-neutron distance. The first limitation can be overcame by using ultra cold neutrons with velocities as small as 5 m/s [50]. These neutrons allow to have minimal recurrence times of order of the second (less than the neutron lifetime and the coherence time) and length of the interferometer of order of meters. The second limitation can be passed by using neutron beams of intensities of the order $I \simeq (10^8 - 10^{10}) n/s$ [51]. Indeed, for neutron velocity of the order of $v \simeq 1$ m/s, a distance $d \simeq 10^{-8}$m is obtained in correspondence with an intensity $I \simeq 10^8$n/s.

In conclusion, we have shown that, in the time evolution of neutrons, the axion mediated fermion-fermion interaction generates a contribution to the total phase. Such a contribution can be in principle detectable, by using ultra cold neutrons in an interferometer in which the two beams are affected by differently oriented magnetic fields, in order that the phase difference depends only by the axion–induced interaction. Significant phase difference is obtained for a wide range of ALP parameters.

Acknowledgements
A.C. and A.Q thank partial financial support from MIUR and INFN. A.C. also thanks the COST Action CA1511 Cosmology and Astrophysics Network for Theoretical Advances and Training Actions (CANTATA). SMG acknowledge support from the European Regional Development Fund for the Competitiveness and Cohesion Operational Programme (KK.01.1.1.06–RBI TWIN SIN) and from the Croatian Science Fund Project No. IP-2016–6–3347 and IP-2019–4–3321. SMG also acknowledge the QuantiXLie Center of Excellence, a project co–financed by the Croatian Government and European Union through the European Regional Development Fund– the Competitiveness and Cohesion Operational Programme (Grant KK.01.1.1.01.0004).

References

[1] Bilenky S M and Pontecorvo B, *Phys. Lett. B* **61**, 248 (1976).
[2] Bilenky S M and Pontecorvo B, *Yad. Fiz.* **3**, 603 (1976).
[3] Nachtmann O, *"Elementary Particle Physics: Concepts and Phenomena"*, Springer, Berlin (1990).
[4] Capolupo A, Lambiase G, and Quaranta A, *Phys. Rev. D*, **101**, 095022 (2020).
[5] Capolupo A, Carloni S and Quaranta A, *Phys. Rev.* D **105**, 105013 (2022).
[6] Capolupo A, Giampaolo S M and Quaranta A, *Phys. Lett.* B **820**, 136489 (2021).
[7] Capolupo A, Giampaolo S M, Hiesmayr B C, Lambiase G and Quaranta A, *J. Phys. G: Nucl. Part. Phys.* **50**, 025001 (2023).
[8] Rubin V, Thonnard W K Jr, Ford N, *The Astrophysical Journal*, **238**: 471, (1980).
[9] Aghanim N et al., Planck Collaboration, *Astron.Astrophys.* **641**, A6, (2020).
[10] Keshavarzi A, Khaw K S and Yoshioka T, *Nucl. Phys.* B **975**, 115675 (2022).
[11] Capolupo A, Lambiase G and Quaranta A, *Phys. Lett.* B **829**, 137128 (2022).
[12] Peccei R D and Quinn H, *Phys. Rev. Lett.* **38**, 1440 (1977).
[13] Peccei R D and Quinn H, *Phys. Rev. D* **16** 1791 (1977).
[14] Weinberg S, *Phys. Rev. Lett.* **40**, 223 (1978).
[15] Wilczek F, *Phys. Rev. Lett.* **40**, 279 (1978).
[16] Raffelt G G, *J. Phys. A* **40**, 6607 (2007).
[17] Ellis J, *Nucl. Phys. A* 827, 187-198 (2009).
[18] Dine M, Fischler W, and Srednicki M, Phys. Lett. B **104**, 199 (1981).
[19] Zhitnitsky A, Sov. J. Nucl. Phys. **31**, 260 (1980).
[20] Particle Data Group Zyla P A et al., *Progress of Theoretical and Experimental Physics*, vol. **2020**, Issue 8, August 2020, 083C01 (2020).
[21] Kim J E, Phys. Rev. Lett. **43**, 103 (1979).
[22] Shifman M A, Vainshtein A, and Zakharov V I, Nucl. Phys. B 1**66**, 493 (1980).
[23] Kim J E and Marsch D J E, *Phys. Rev. D* **93**, 025027 (2016).
[24] De Martino I, Broadhurst T, Henry-Tye S-H, Chiueh T, Schive H-Y and Lazkoz R, *Phys. Rev. Lett.* **119**, 221103 (2017).
[25] Rubakov V A, *JETP Lett.* **65**, 621-624 (1997).
[26] Marsch D J E, *Phys. Rep.*, **643**, 1 (2016).
[27] Zavattini E et al. (PVLAS Collaboration), *Phys. Rev. D* **77**, 032006 (2008).
[28] Pugnat P et al. (OSQAR Collaboration), *Phys. Rev. D* **78**, 092003 (2008).
[29] Ballou R et al. (OSQAR Collaboration), *Phys. Rev. D* **92**, 092002 (2015).

Journal of Physics: Conference Series **2533** (2023) 012044 doi:10.1088/1742-6596/2533/1/012044

[30] Ehret K et al. (ALPS Collaboration), *Phys. Lett. B* **689**, issues 4-5, pages 149-155 (2010).
[31] Aune S et al. (CAST Collaboration), *Phys. Rev. Lett.* **107**, 261302 (2011).
[32] Du N et al. (ADMX Collaboration), *Phys. Rev. Lett.* **120**, 151301 (2018).
[33] Barbieri R et al., *Phys. Dark Univ.* **15**, 135-141 (2017).
[34] Capolupo A, Lambiase G, Vitiello G, *Adv. In High En. Phys.* 826051 (2015).
[35] Capolupo A, De Martino I, Lambiase G, Stabile A, *Phys. Lett. B* **790**, 427-435 (2019).
[36] Moody J E, Wilczek F, *Phys. Rev. D*, **30**, 130 (1984).
[37] Daido R, Takahashi F, *Phys. Lett. B*, **772**, 127 (2017).
[38] Bezerra V B, Klimchitskaya G L and Mostepanenko V M and Romero C, *Eur. Phys. J. C* **74**, 2859 (2014).
[39] Klimchitskaya G L and Mostepanenko V M, *Phys. Rev. D* **95** 123013 (2017).
[40] Klimchitskaya G L and Mostepanenko V M, *Eur. Phys. J. C* **75**, 164 (2015).
[41] Capolupo A, Giampaolo S M, Lambiase G, Quaranta A, *Phys. Lett. B* **804**, 135407 (2020).
[42] Rauch H, Werner S A, *Neutron Interferometry–Lessons in Experimental Quantum Mechanics, Wave–Particle Duality, and Entanglement*, 2nd Edition, Oxford University Press, Oxford (2015).
[43] Werner S A, Staudenmann J–L, Colella R, *Phys. Rev. Lett.*, **42**, 1103 (1979).
[44] Allman B E, Kaiser H, Werner S A, Wagh A G, Rakhecha V C, Summhammer J, *Phys. Rev. A*, **56**, 4420 (1997).
[45] Wagh A G, Rakhecha V C, *Phys. Lett. A*, **148**, Issues 1–2, pp. 17-19 (1990).
[46] Wagh A G, Rakhecha V C, Fischer P, Ioffe A, *Phys. Rev. Lett.*, **81**, 1992 (1998).
[47] Capolupo A, Giampaolo S M, Quaranta A, Neutron interferometry, fifth force and axion like particles, European Physical Journal C, **81**, 1116 (2021)
[48] Ott F, Kozhevnikov S, Thiaville A, Torrejon J, Vazquez M, *Nucl. Inst. Meth. in Phys. Res. A*, **788** (2015), pp. 29-34.
[49] Gradshteyn I S, Ryzhik I M, *Table of Integrals, Series and Products*, 7th edition, Academic Press (2007), pp. 110-111.
[50] Steyerl A, *Phys. Lett. B*, **29**, Issue 1, pp. 33-35 (1969).
[51] INTERNATIONAL ATOMIC ENERGY AGENCY, *Compendium of Neutron Beam Facilities for High Precision Nuclear Data Measurements*, IAEA-TECDOC-1743, IAEA, Vienna (2014).